

Wood Classification Study based on Thermal Physical Parameters with Intelligent Method of Artificial Neural Networks

Shubo Cao,^a Shiyu Zhou,^{b,*} Jiying Liu,^b Xiaoping Liu,^c and Yucheng Zhou^a

In this study, 65 kinds of wood samples were classified by using artificial neural networks based on the measured value of wood thermal physical parameters. First, the thermal conductivities and the thermal diffusion coefficients of the wood samples were measured. The transient temperature rise curve of wood samples during the test process was recorded, and the characteristic values of the transient temperature rise curve were extracted by logarithmic curve fitting. The emissivity spectrum representing the thermal physical properties of wood surface was measured, and the characteristic spectral data were selected according to the principal component analysis. An artificial neural network model was established based on the extracted feature values and characteristic spectral data to classify the wood species. The experimental results showed that the comprehensive correct classification rate of the proposed wood classification method was 99.85%. In addition, the proposed wood classification method was compared with a wood classification method based on laser induced breakdown spectrum and near infrared spectrum, which indicates the feasibility of wood classification based on the values of wood thermal physical properties.

DOI: 10.15376/biores.17.1.1187-1204

Keywords: Wood species classification; Thermal conductivity; Artificial neural network

Contact information: a: School of Information and Electrical Engineering, Shandong Jianzhu University, Jinan, China; b: School of Thermal Engineering, Shandong Jianzhu University, Jinan 250101, China; c: The Faculty of Engineering, Lakehead University, Thunder Bay, ON P7B 5E1, Canada;

* Corresponding author: zhou-1sy@163.com

INTRODUCTION

Wood has a wide range of applications in human life. It can be processed into a variety of products because different kinds of wood have various physical and chemical properties. Therefore, wood identification has become a significant factor in the wood industry. It plays an important role in wood import-export trade business, scientific research, processing technology, archaeological work, precious wood identification, *etc.* In early classification work, wood species were differentiated by the macroscopic or microscopic characteristics. Most of these methods are time consuming, inconvenient, or inaccurate.

With the development of digital image algorithms, visual image features can be used to identify wood species, and some digital image algorithms such as gray-level co-occurrence matrices and edge detection for extracting wood surface features have been proposed (Tou *et al.* 2008; Ristiawanto *et al.* 2019). Zhao *et al.* (2014) converted some wood color images into V1V2I color-based images and identified wood species by

comparing the established model with the histogram curves of specimens. Liu *et al.* (2020) presented a split shuffle residual (SSR)-based convolutional neural network (CNN) that learns features automatically from wood images, allowing real-time classification of rubber wood boards. Another commonly used method for wood classification is the analysis of wood microstructure through digital image processing technology. Based on scanning electron microscopy, Kita *et al.* (2020) suggested a new method to measure the microfiber angles by using polarization microscope, and then a multivariate classifier was used to convert them into a two-dimensional correlated-map for wood classification.

Because the near-infrared (NIR) spectrum of wood contains the information of wood chemical properties, NIR spectroscopy has been developed in wood classification. Park *et al.* (2017) investigated the interrelationship between wood chemical compositions and the NIR spectrum with traditional wet chemistry methods and infrared spectral analyses, providing a basis for wood classification. Santos *et al.* (2020) analyzed the NIR spectrum of wood samples belong to four different species; the effects of three different pretreatment methods on classification accuracy were compared. Feng *et al.* (2020) used support vector machine (SVM) and Markov distance to identify the mid-infrared spectra of 5 kinds of wood. The recognition rate of SVM was slightly higher than that of Markov distance, while the correct recognition rate of SVM with smoothing plus first derivative processing was 98%. By combining the NIR spectrum of wood with a variety of pattern recognition methods, Hao *et al.* (2019) compared the influence of different methods on the wood recognition accuracy. The soft independent modeling of class analogy (SIMCA) model after 5-point smoothing or wavelet derivative (WD) pretreatment of wood spectrum achieved the best recognition rate. Pozhidaev *et al.* (2019) considered single-reflection attenuated total reflection IR spectroscopy to classify 53 coniferous wood samples and 77 deciduous wood samples. However, the peaks of different wood chemical compositions are weak and sometimes overlap in the near-infrared range, which reduces the correct recognition rate, thus restricting its application.

Compared with other materials analysis techniques, wood specific emissivity spectroscopy has the unique advantages of fast speed, simple sample preparation, and low source interference. Specific emissivity spectroscopy has been widely used in materials, thermal radiation, and photovoltaic power generation (Budaev and Bogy 2011; Gibelli *et al.* 2017; Sako *et al.* 2021). In addition, the thermal conductivity coefficient and thermal diffusion coefficient of wood are the pivotal parameters for basic research, analysis, and engineering design in the field of wood application (Adili *et al.* 2016). The thermal physical parameters of wood include the information of internal physical properties of wood, while the emissivity spectrum of wood includes the information of surface physical properties of wood. However, there are few studies about the classification of wood species based on wood thermal physical parameters and emissivity spectroscopy.

In this study, the emissivity spectra, thermal conductivity, and thermal diffusivity of 65 species of wood were measured to create a dataset of wood thermal physical properties. The established dataset is a benchmark to evaluate the performance of the proposed method and also provides a reference for future research.

A novel classification method for wood species identification was proposed. The method considered the differences of thermal properties (thermal conductivity, thermal diffusion coefficient) and specific emissivity of different wood species under the same experimental conditions. Such an approach has never been applied to wood classification. Principal component analysis (PCA) and logarithmic curve feature extraction were used to extract wood characteristic spectral data and thermal physical parameter data, respectively.

An artificial neural network model was established to identify wood species using the extracted data as inputs.

EXPERIMENTAL

Sample Preparation

Samples were taken from 65 kinds of wood belonging to 4 families. Each kind of wood was composed of 5 pieces of samples, for a total of 325 pieces of wood. One piece of each wood sample was randomly selected as the main sample, and the other four pieces were used as the sub-samples. Therefore, the total number of the main samples was 65, and the total number of sub-samples was 260. The production of an experimental sample is shown in Fig. 1. As shown in Fig. 2, the experimental sample used to measure the specific emissivity spectrum was disc-shaped with a diameter and thickness of 18 mm and 2 mm, respectively. As shown in Fig. 3, the experimental samples used for measuring thermal conductivity and thermal diffusion coefficient were two uniform rectangular samples whose sizes were 50 mm × 50 mm × 20 mm.

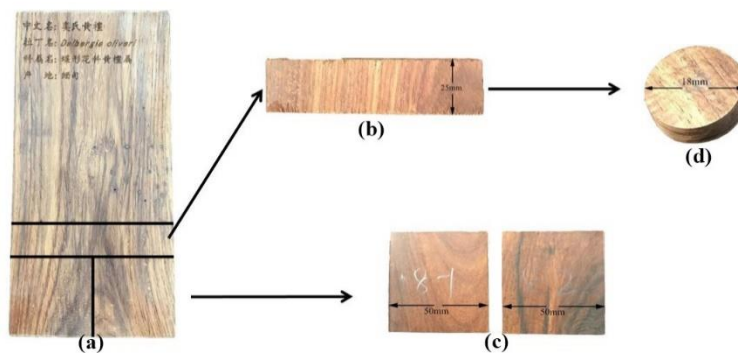


Fig. 1. Production of the experimental samples

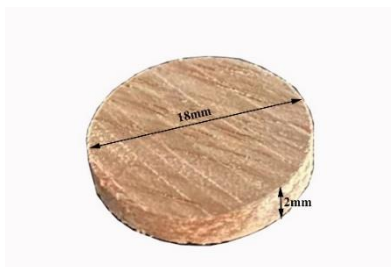


Fig. 2. Specimen for measuring the emissivity



Fig. 3. Specimen for measuring thermal conductivity

The wood samples were stored in an air-conditioned room kept at 26 °C and 55% humidity. All wood samples were oven-dried before testing to avoid the influence of moisture content on the measured values.

Experimental Principle and Method

In this paper, the thermal conductivity and the thermal diffusion coefficient of wood samples were measured by Hot Disk thermal constant analyzer TPS2200 (Hot Disk, Sweden Ltd, Gothenburg, Sweden). The experimental device was composed of the voltage stabilizer, the computer, Hot Disk host, and the probe bracket (Fig. 4). The measurement principle of Hot Disk was the transient plane heat source method (Trofimov *et al.* 2020). The core element of Hot Disk measurement was a temperature dependent probe with a continuous double helix structure. The outer layer of the probe was a double-layer Kapton protective layer, as shown in Fig. 5(a).

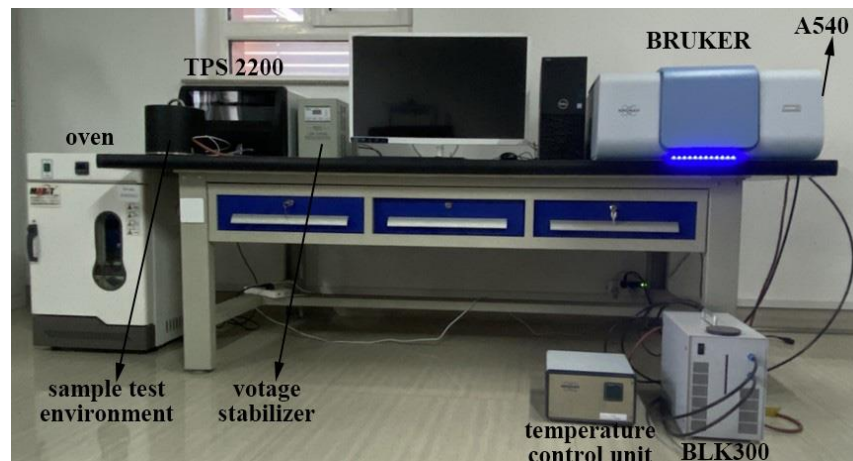


Fig. 4. Experimental facilities used in this study

It is necessary to take the specific heat volume of the samples as a known input when measuring the thermal conductivity and thermal diffusion coefficient of wood samples. Therefore, the volume specific heat of the samples should be measured first. The volume specific heat of the samples was measured by the Specific Heat Capacity Module of the Hot Disk thermal constant analyzer. The core component of the volume specific heat measurement of wood samples was a gold vessel probe with the diameter of 20 mm and the height of 5 mm. To avoid heat exchange between the gold vessel probe and the external environment during the experiment, two sponge blocks were used to wrap the probe, as shown in Fig. 5(b).

After the measurement of the sample volume specific heat, the thermal conductivity and thermal diffusion coefficient of the samples were measured. The anisotropic module of the Hot Disk thermal constant analyzer was used in the experiment. The specific experimental process for measuring the thermal conductivity and thermal diffusion coefficient is as follows. As shown in Fig. 5(c), the probe was placed between the two fixed rectangular wood samples, and parameters such as the volume specific heat of the sample were input into the anisotropic module as known conditions.

All the tested samples used in the experiment were tested in turn. Specifically, for 65 kinds of main samples, the samples were replaced after each experiment, with an interval of 5 min, which is enough to restore the probe temperature to the initial temperature and conduct two rounds of tests. The time interval between the second test of the same sample and the last test was at least $65 * 5 = 325$ min, which is sufficient for the sample temperature to recover to the initial temperature. Similar to the main sample, the sub-sample was tested for 4 rounds. In addition, the initial environmental conditions for each test were the same. It is emphasized that the thermal diffusivity coefficients used in this paper are calculated by the Hot Disk method.

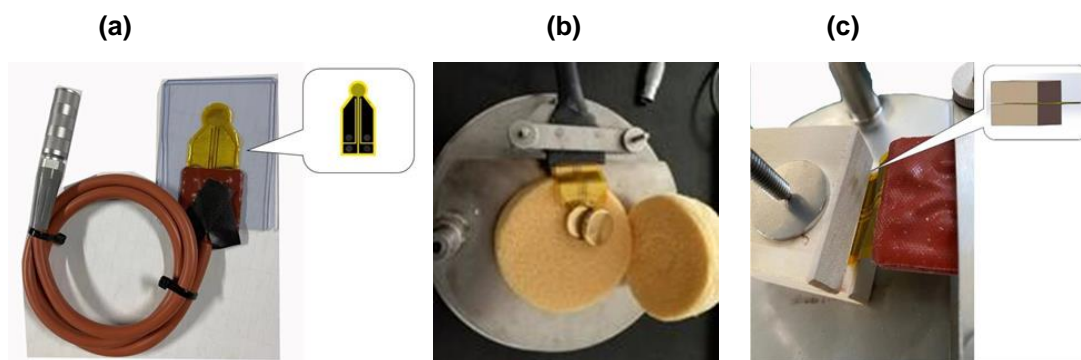


Fig. 5. (a) The metal probe used in the experiment; (b) The gold vessel probe used in the experiment; (c) Schematic diagram of sample placement

The experimental apparatus for measuring emissivity spectrum of wood samples included Bruker Fourier infrared spectrometer (Karlsruhe, Germany), temperature control unit, and heat exchanger BLK300 (Fig. 4). During the experiment, the wood sample was placed in the transmitting adapter A540 (Fig. 7). The emissivity spectrum was measured by Fourier infrared spectrometer and then displayed on the computer. The temperature control unit was applied for heating the sample to the specified temperature, and the heat exchanger BLK300 was used to keep the wood sample temperature stable.

The measurement of emissivity spectrum for wood samples was based on the basic principle of radiation heat transfer. At the beginning of the experiment, it is necessary to heat the wood sample to 400 K (120 °C) and keep it at a stable level. According to the Planck law, the blackbody radiation force reaches the maximum value in the range of 6000 nm to 10000 nm at the temperature of 400 K. Therefore, to obtain the stable specific emissivity spectrum of wood samples, the experimental wavelength range was set as 4200 to 50000 nm, and the sampling interval was set as 20.13 nm^{-1} . The specific experimental process of measuring the emissivity spectrum of the sample was as follows. As shown in Fig. 7, the sample was placed in the sample clip, fixed on the emission adapter A540, heated to the set temperature, and left for 10 min. The background single-channel spectral was measured to provide a benchmark for computation. Finally, the emissivity spectra of the

wood samples were obtained by measuring the single channel spectra of the wood samples. Each spectrum was consisted by 2,281 discrete points with the resolution of 4 cm^{-1} and the scanning speed of 5 kHz.

The wavelength range of near-infrared spectrum is 750 to 2500 nm, mid-infrared spectrum is 2500 to 25,000 nm, and the wavelength range above 25,000 nm is far-infrared spectrum. Therefore, the emissivity spectrum measured at 4200 to 50,000 nm in this paper belongs to the middle-far infrared range. The commonly used method of wood identification by near infrared spectroscopy is based on the chemical composition differences of different tree species. In this study, tree species were classified based on the thermal physical characteristics of wood, using mid-far infrared wavelengths, which are also the concentrated region of emissivity spectrum.

In this paper, the emissivity spectra of 65 species of wood were measured. For 5 samples (one set of main samples and four sets of sub-samples) of each wood, 10 specific emissivity spectra were obtained, totaling 650 emissivity spectra. During model training, 520 groups of feature extraction data of subsamples were taken as the training set, and 130 groups of feature extraction data of main samples were taken as the verification set. Figure 6 shows 10 specific emissivity spectra of experiments on *Pterocarpus macrocarpus*. The enlarged part in Fig. 6 is the part of the spectrum that is less disturbed by noise. The abscissa is the wave number (cm^{-1}), and the ordinate represents the emissivity (%).

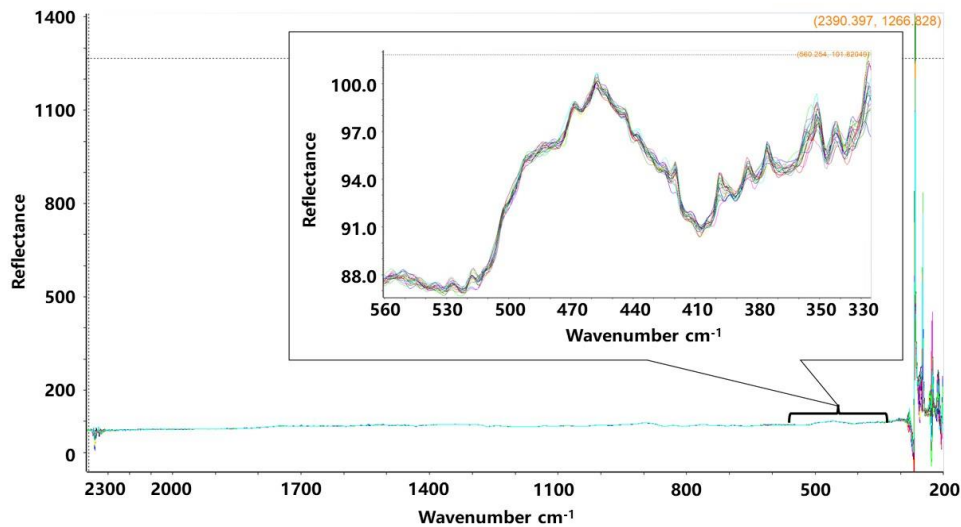


Fig. 6. Schematic diagram of specific emissivity spectrum for *Pterocarpus macrocarpus*



Fig. 7. The transmitting adapter A540

Data Processing And Model Training

Feature extraction

In the test of thermal physical property parameters, 5 samples of each wood were evaluated, and each group of experiments required an interval of 60 min, which required a long time to complete the experiment. In addition, the calculation formula of D_{τ} is not clear, and the value of D_{τ} cannot be calculated accurately. Therefore, the transient temperature rise curve collected during the experiment was used to replace the thermal physical parameters of the experimental samples for model training. However, the number of data obtained for each curve was so numerous that it was necessary to extract the feature values from these data. As shown in Fig. 8, which was the temperature rise curve of the measured wood sample, if all the temperature data were taken as the model input, it would be hard to obtain an effective model. Therefore, a mathematic curve was used to fit the transient temperature rise curve in this study, as shown in Eq. 1,

$$\Delta T = a \ln(t) + b \quad (1)$$

where ΔT represents the temperature increment, t represents time, a and b are undetermined parameters, *i.e.*, the characteristic value of the transient temperature rise curve. All the experimental results were fitted, and the fitting degrees of these curves are all above 0.98, demonstrating the validity of the fitting formula. Some of the fitting results are shown in Fig. 9. The detailed extracted feature values of *Pterocarpus macrocarpus* are shown in Table 1.

Table 1. Detailed Extracted Feature Values of *Pterocarpus macrocarpus*

| | Emissivity Spectral Characteristics | | | Thermal Physical Characteristics | |
|---|-------------------------------------|------------|------------|----------------------------------|------------|
| 1 | 0.7193045 | -0.4731353 | -0.0604565 | 0.0547555 | -0.0494429 |
| | 0.7116342 | -0.4957342 | -0.0393647 | 0.0657513 | -0.0552398 |
| 2 | 0.7110340 | -0.5029993 | -0.0245182 | 0.0591802 | -0.0477010 |
| | 0.7113333 | -0.4734103 | -0.0254569 | 0.0524822 | -0.0539498 |
| 3 | 0.7135605 | -0.4260158 | -0.0242757 | 0.0590561 | -0.0544432 |
| | 0.7140434 | -0.4141391 | -0.0255731 | 0.0565322 | -0.0568444 |
| 4 | 0.7132047 | -0.3447801 | -0.0194827 | 0.0566388 | -0.0503004 |
| | 0.7136665 | -0.3291264 | -0.0214502 | 0.0560758 | -0.0578149 |
| 5 | 0.7131303 | -0.2854434 | -0.0350699 | 0.0599563 | -0.0530138 |
| | 0.7130286 | -0.2681826 | -0.0270840 | 0.0577767 | -0.0539641 |

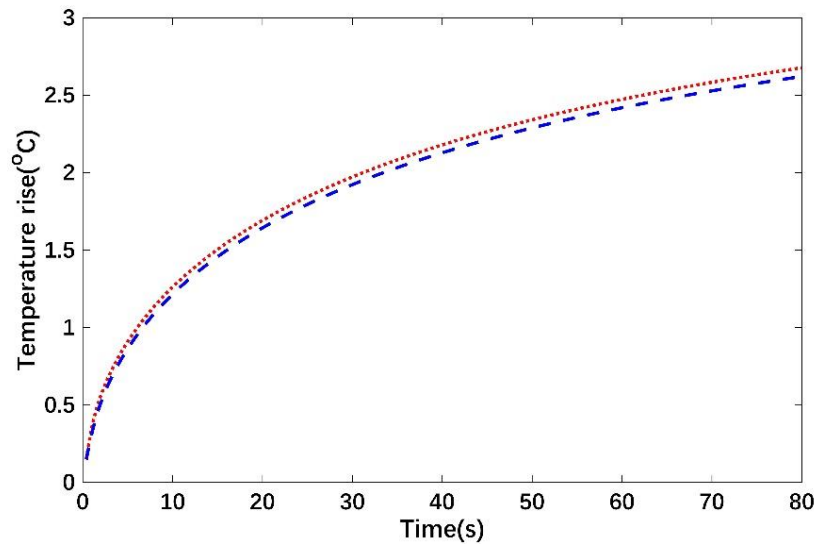


Fig. 8. Temperature rise schematic diagram of the experimental sample

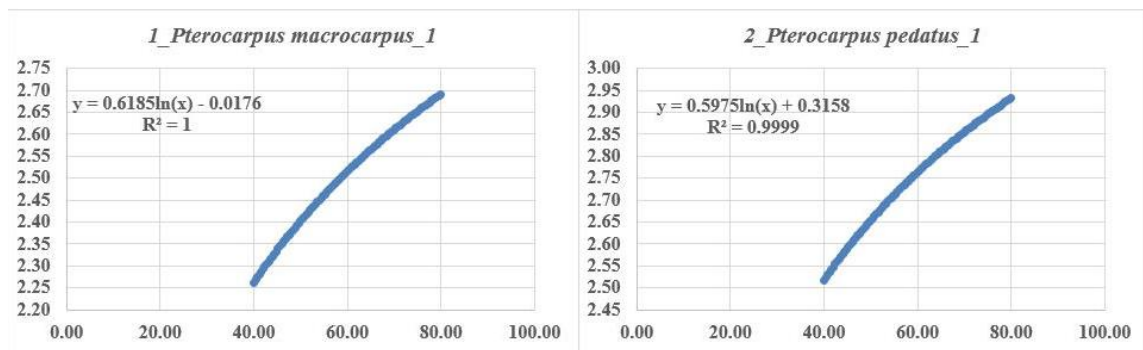


Fig. 9. Part of the fitting results of the temperature rise curves

Principal component analysis (PCA) is a widely used data dimensionality reduction method. The main idea of PCA is to map n -dimensional features to k -dimensional orthogonal features. First, it is necessary to select a part of the spectral spectrum that is less disturbed by noise in the emissivity spectrum obtained from the experiment. In this paper, the emissivity spectrum with the wavelength range of 3000 to 10500 nm was selected as the characteristic spectrum of experimental wood samples, with a total of 651 sample points. PCA processing was carried out for all the characteristic spectra, and the top three features that with principal component scores were taken as the input values of the model. The PCA results of characteristic spectrum are shown in Fig. 10.

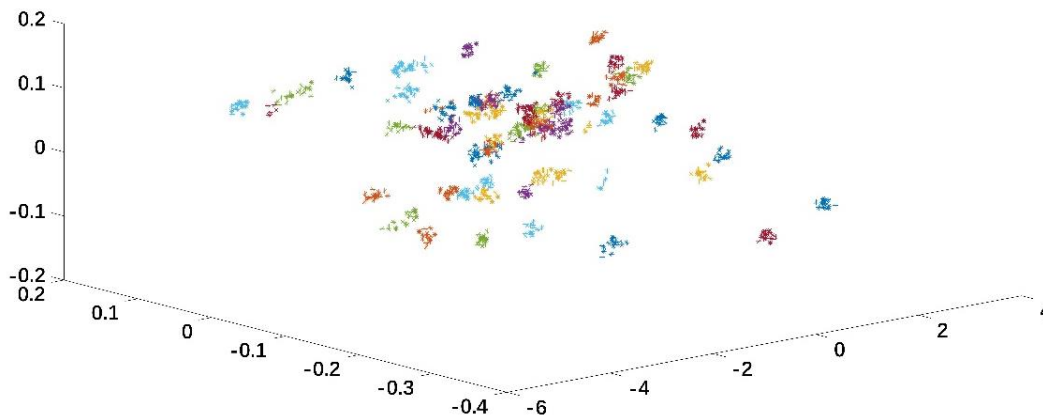


Fig. 10. PCA results of the characteristic spectrum

Classification modeling

Back propagation neural network (BPNN) is an effective neural network model, which is mainly characterized by forward transmission of signals and backward propagation of errors. By constantly adjusting the weight value of the network, the output of the network could be as close as possible to the expected value, so as to realize the training of model. The two characteristic parameters of transient temperature rise curve and three characteristics of emissivity spectrum for wood experimental samples depicted in the previous section were taken as input layer parameters of BPNN, and the number of wood categories was taken as output layer parameters. As shown in Table 2, the tansig function and the logsig function were used in the hidden layers and the input layer, respectively. The transfer function of the purelin and the trainlm were used as the output layer activation function and the BP neural network training function, respectively. The maximum number of training was set to 1000, while the training error goal was 10^{-9} and the learning rate was 0.1. The remaining training parameters were kept to the default values. In this paper, MATLAB R2021a was used for model training.

Table 2. Parameters of the BP Neural Network

| | Structure | Parameters |
|---|------------------------------------|---------------------|
| 1 | the hidden layer transfer function | the tansig function |
| 2 | the input layer neurons | the logsig function |
| 3 | the maximum training times | 1000 |
| 4 | the maximum training error | 10^{-9} |
| 5 | the learning rate | 0.1 |

RESULTS AND DISCUSSION

The effectiveness of the proposed wood classification model based on wood thermal physical characteristics was validated by comparing different featured inputs and different modeling methods. The wood classification model established in this study was compared with the wood classification model based on laser induced breakdown spectrum (Cui *et al.* 2019) and that based on near infrared spectrum (Yang *et al.* 2019).

Comparison of Different Input Types

The thermal physical constants for 65 kinds of wood samples were measured by Hot Disk thermal constant analyzer and Bruker Fourier infrared spectrometer. For each wood sample, 10 transient temperature rise curves and 10 emissivity spectrums were collected. After the feature extraction process, 50 characteristic values than could reflect the internal and surface thermal physical information of the experimental wood were obtained. For each of 65 wood species, 5 groups of samples were selected for the experiment, with one group of samples as the main sample and the other 4 groups as sub-samples, totaling 325 groups of samples. For each group of main samples, two thermal physical property experiments and emissivity spectral test experiments were conducted, and a total of 130 groups of experimental data were generated from the main samples. Two samples were randomly selected from each sub-sample group for 4 thermal physical property experiments, and the remaining two samples were used for emissivity spectrum measurement. The same 4 repeated experiments were conducted to generate a total of 520 groups of experimental data. A total of 650 sets of experimental data were collected for the main sample and sub-samples. During model training, 520 groups of feature extraction data of sub-samples were used as training sets, and 130 groups of feature extraction data of main samples were used as verification sets.

After the data division and model training process, a classification model was established with wood thermal physical property characteristics as input variables. As shown in Fig. 11, the CCR of the validation set was 100%. A ten-fold cross validation was performed on the experimental data. This means that the experimental data were divided into 10 pieces on average, among which 9 pieces were randomly selected as training data and the remaining 1 piece was used as validation data. Each piece of data was deemed as validation data for once, so there were 10 times of model training were conducted in the cross validation process. The results of cross validation were shown in Fig. 12 (M1). Among the 10 results, the maximum value of the correct classification rate (CCR) was 100%, while the minimum CCR is 99.23% and the average CCR was 99.85%.

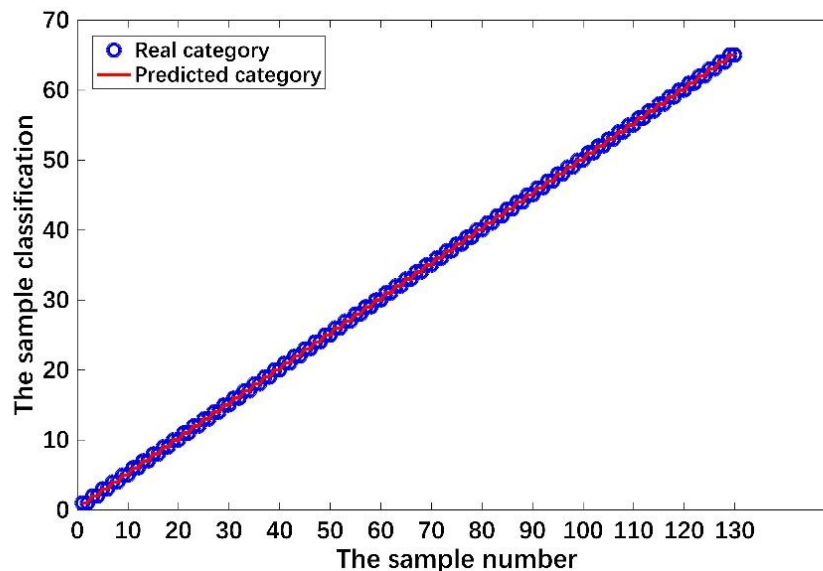


Fig. 11. Validation results of the wood classification model

To verify the superiority of the M1 method, the thermal property characteristics and emissivity spectral characteristics of wood were separately used as input variables for cross validation, and then the results were compared with the M1 method. M1 represents the classification model based on wood thermal physical properties and emissivity spectral characteristics. M2 represents the classification model based on the thermal properties of wood alone. M3 represents the classification model trained with emissivity spectral characteristics alone.

The results of cross validation are shown in Fig. 12 and Table 3. Among the 10 times cross validation results of M2, the maximum CCR was 99.23%, while the minimum value was 70% and the average value was 95.15%. In the cross validation experiments of M3, the maximum CCR is 99.23%, while the minimum value and the average value were 73.85% and 95.54%, respectively. By comparison, the accuracy of classification was significantly improved by the combination of the two characteristics.

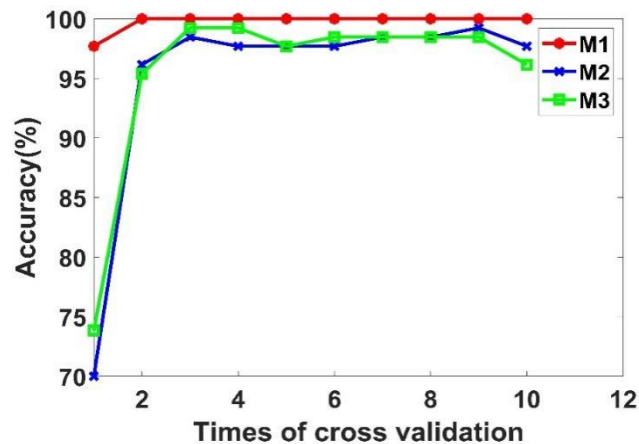


Fig. 12. Comparison of ten-fold cross validation results of M1, M2 and M3

Table 3. Detailed Errors of Cross-Validation of M1, M2, and M3

| | M1 | M2 | M3 |
|----------------------|-------|-------|-------|
| Maximum accuracy (%) | 100 | 99.23 | 99.23 |
| Minimum accuracy (%) | 99.23 | 70 | 73.85 |
| Average accuracy (%) | 99.77 | 95.15 | 95.54 |

To verify the advantages of the logarithmic curve fitting feature extraction method, the experimental wood thermal physical parameters (radial/chord wise thermal conductivity, radial/chord wise thermal diffusivity) and emissivity spectral features were used as input variables for the training of cross validation model (M4). The ten-fold cross validation results of M1 were compared with that of M4, as shown in Fig. 13. The detailed CCRs of the two models are listed in Table 4.

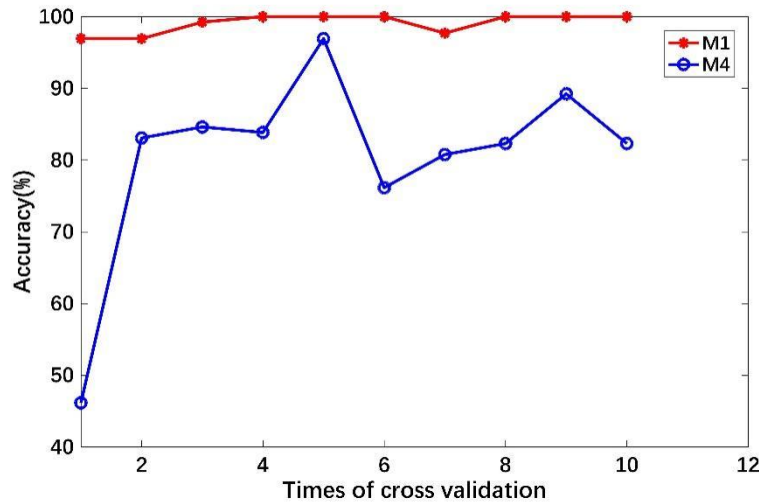


Fig. 13. Comparison of ten-fold cross validation results of M1 and M4

The comparison results show that the CCRs of M1 were higher than that of M4. The averages CCR for M1 and M4 were 99.85% and 80.54%, respectively. In addition, the fluctuation of the CCRs of model based on M4 was higher than that of M1. The CCRs for M1 were from 96.92% to 100% and those of M4 were from 46.15% to 80.54%, respectively.

Table 4. Comparison of Ten-fold Cross Validation Results between M1 and M4

| Input Variable Type | Correct Classification Rate (%) | | |
|---------------------|---------------------------------|-------|---------|
| | Max | Min | Average |
| M1 | 100 | 96.92 | 99.85 |
| M4 | 96.92 | 46.15 | 80.54 |

In order to verify the fact that the identification accuracy of the data extracted with emissivity spectral features was higher than that using single data, the M3 method was compared with the wood identification model using the characteristic values with the highest score of the data extracted with emissivity spectral features as the input variable (M5). The cross-validation results of M3 and M5 were compared, as shown in Fig. 14. The detailed CCRs of the two models are listed in Table 5.

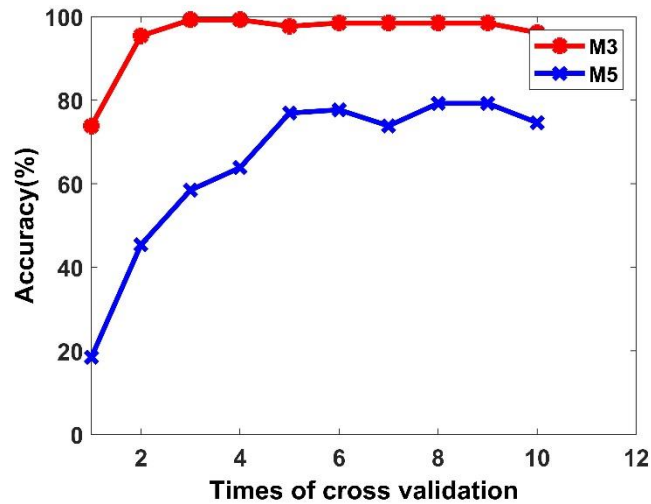


Fig. 14. Comparison of ten-fold cross validation results of M3 and M5

The comparison results show that the CCRs of M3 were higher than that of M5. The averages CCR for M1 and M4 were 99.85% and 80.54%, respectively. In addition, the fluctuation of the CCRs of model based on M4 was higher than that of M1. The CCRs for M1 are from 96.92% to 100% and that of M4 are from 46.15% to 80.54%, respectively. Since the emissivity spectrum can characterize the thermal physical properties of wood surface, adding this factor was equivalent to increasing the characterization parameters of wood samples, rather than merely adding a principal factor whose effect cannot be replaced by conventional principal factors.

Table 5. Comparison of Ten-fold Cross Validation Results between M3 and M5

| Input Variable Type | Correct Classification Rate (%) | | |
|---------------------|---------------------------------|-------|---------|
| | Max | Min | Average |
| M3 | 99.23 | 73.85 | 95.54 |
| M5 | 79.23 | 18.46 | 64.77 |

Comparison of Different Models

In this section, the proposed wood classification model based on thermal physical parameters (TP) was compared with a wood classification model based on laser induced breakdown spectrum (LIBS) (Cui *et al.* 2019) and a wood classification model based on near infrared spectrum (NIR) (Yang *et al.* 2019). Xu *et al.* (2019) used laser induced breakdown spectroscopy combined with artificial neural network to classify 4 kinds of wood samples. Yang *et al.* (2019) used near infrared spectroscopy combined with LeNet3 to classify 5 kinds of softwood samples.

The average CCR of the classification model based on laser induced break-down spectrum (Cui *et al.* 2019) and the classification model based on near infrared spectrum (Yang *et al.* 2019) were 99.17% and 95.19% for 10-fold cross validation, respectively. The average CCR of the proposed classification model based on wood thermal physical property and emissivity spectral characteristics was 99.85%. The CCR of cross validation for the above three methods is shown in Table 6. The classification model proposed in this study is superior to the other mentioned two models. In addition, the method in Cui *et al.* (2019) and Yang *et al.* (2019) only studied the classification model for up to 5 kinds of

wood, while 65 kinds of common wood were classified in this study. The classification model was more complex than that of the other two classification models, which also reflected the superiority of the proposed wood classification model.

Table 6. Correct Classification Rate of Ten-fold Cross Validation for Different Methods

| Method | Species | Correct classification rate (%) | | |
|-------------------------------|---------|---------------------------------|-------|---------|
| | | Max | Min | Average |
| LIBS (Cui <i>et al.</i> 2019) | 4 | 99.17 | 96.67 | 98.08 |
| NIR (Yang <i>et al.</i> 2019) | 5 | 100 | 89.71 | 95.19 |
| TP (present study) | 65 | 100 | 96.92 | 99.85 |

CONCLUSIONS

1. A novel method for wood classification was put forward. The method was established based on the thermal physical information and spectral characteristics of specific emissivity of different wood species.
2. The anisotropic (axial and chord wise) thermal conductivity and thermal diffusivity, which represent the internal thermal physical properties of wood, were measured. The established dataset could be used not only as a benchmark to evaluate the performance of the proposed method, but also provided a reference for the future research.
3. The feature extraction data are used as the input data of BPNN, so as to establish a classification model of wood species. In order to verify the effectiveness of the proposed method, 65 kinds of common wood were tested in this work. The experimental results showed that the average correct classification rate of the proposed wood classification method was 99.85%, which indicates the feasibility of wood classification model based on wood thermal physical properties.
4. In addition, the proposed wood classification method was compared with a wood classification method based on laser induced breakdown spectrum and near infrared spectrum, which indicated the feasibility of wood classification based on the values of wood thermal physical properties. Future work will focus on improving the calculation speed of wood classification model, so as to satisfy the requirements of real-time classification work.

ACKNOWLEDGMENTS

The research was supported by the Taishan Scholar Project of Shandong Province of China under Grant 2015162. This work was also supported by the Plan of Introduction and Cultivation for Young Innovative Talents in Colleges and Universities of Shandong Province.

REFERENCES CITED

- Adili, A., Lachheb, M., Brayek, A., Guizani, A., and Ben Nasrallah, S. (2016). "Estimation of thermophysical properties of lightweight mortars made of wood shavings and expanded polystyrene beads using a hybrid algorithm," *Energy and Buildings* 118(15), 133-141. DOI: 10.1016/j.enbuild.2016.02.039
- Budaev, B. V., and Bogy, D. B. (2011). "Extension of Planck's law of thermal radiation to systems with a steady heat flux," *Annalen Der Physik* 523(10), 791-804. DOI: 10.1002/andp.201100135
- Cui, X., Wang, Q., Zhao, Y., Qiao, X., and Teng, G. (2019). "Laser-induced breakdown spectroscopy (LIBS) for classification of wood species integrated with artificial neural network (ANN)," *Applied Physics* 125(4), 1-12. DOI: 10.1007/s00340-019-7166-3
- Feng, G., Zhu, Y., and Li, Y. (2020). "Identification method of imported timber species by mid-infrared spectrum," *Spectroscopy and Spectral Analysis* 40(7), 2128-2132. DOI: 10.3964/j.isn.1000-0593(2020)07-2128-05
- Gibelli, F., Lombez, L., and Guillemoles, J. F. (2017). "Absorption coefficient and non-equilibrium generalized Planck's law for improved hot carrier photoluminescence spectroscopy," in: *IEEE 44th Photovoltaic Specialist Conference*, Washington, DC, , pp. 1-3.
- Hao, Y., Shang, Q., Yao, M., and Hu, Y. (2019). "Identification of wood species based on near infrared spectroscopy and pattern recognition method," *Spectroscopy and Spectral Analysis* 39(3), 705-710(2019). DOI: 10.3964/j.isn.1000-0593(2019)03-0705-06
- Kita, Y., Mizuno-Tazuru, S., and Sugiyama, J. (2020). "Two-dimensional microfibril angle mapping via polarization microscopy for wood classification," in: *International Conference on Forest Products*, Bogor, Indonesia, pp. 12-28.
- Liu, S., Jiang, W., Wu, L., He, W., Min, L., and Wang, Y. (2020). "Real-time classification of rubber wood boards using an SSR-based CNN," *IEEE Transactions on Instrumentation and Measurement* 69(11), 8725-34. DOI: 10.1109/TIM.2020.3001370
- Park, S. Y., Kim, J. C., and Kim, J. H. (2017). "Possibility of wood classification in Korean softwood species using near-infrared spectroscopy based on their chemical compositions," *Journal of the Korean Wood Science & Technology* 45(2), 202-212. DOI: 10.5658/WOOD.2017.45.2.202
- Pozhidaev, V. M., Retivov, V. M., Panarina, E. I., Sergeeva, Y. E., Zhdanovich, O. A., and Yatsishina, E. B. (2019). "Development of a method for identifying wood species in archaeological materials by IR spectroscopy," *Journal of Analytical Chemistry* 74(12), 1192-1201. DOI: 10.1134/S1061934819120104
- Ristiawanto, V., Irawan, B., and Setianingsih, C. (2019). "Wood classification with transfer learning method and bottleneck features," in: *2019 International Conference on Information and Communications Technology*, Yogyakarta, Indonesia, pp. 111-116.
- Sako, E. Y., Orsolini, H. D., Moreira, M., De Sousa Meneses, D., and Pandolfelli, V. C. (2021). "Emissivity of spinel and titanate structures aiming at the development of industrial high-temperature ceramic coatings," *Journal of the European Ceramic Society* 41(4), 2958-2967. DOI: 10.1016/j.jeurceramsoc.2020.11.010
- Santos, J. X., Vieira, H. C., Silva, E. L., Muñiz, G. I. B., Soffiatti, P., and Nisgoski, S.

- (2020). "Near infrared spectroscopy for separation of Tauari wood in Brazilian Amazon native forest," *Journal of Tropical Forest Science* 32(3), 227-236. DOI: 10.26525/JTFS2020.32.3.227
- Te, M., Inagaki, T., Ban, M., and Tsuchikawa, S. (2018). "Rapid identification of wood species by near-infrared spatially resolved spectroscopy (NIR-SRS) based on hyperspectral imaging (HSI)," *Holzforschung* 73(4), 323-30. DOI: 10.1515/hf-2018-0128
- Tou, J. Y., Tay, Y. H., and Lau, P. Y. (2008). "Gabor filters as feature images for covariance matrix on texture classification problem," in: *15th International Conference on Neuro-Information Processing*, Auckland, New Zealand, pp. 745-751.
- Trofimov, A., Atchley, J., Shrestha, S., Desjarlais, A., and Wang, H. (2020). "Evaluation of measuring thermal conductivity of isotropic and anisotropic thermally insulating materials by transient plane source (hot disk) technique," *Journal of Porous Materials* 27(6), 1791-1800. DOI: 10.1007/s10934-020-00956-3
- Yang, S., Lee, H., Park, Y., Chung, H., Kim, H., Park, S., Choi, I., Kwon, O., and Yeo, H. (2019). "Wood species classification utilizing ensembles of convolutional neural networks established by near-infrared spectra and images acquired from Korean softwood lumber," *Journal of the Korean Wood Science and Technology* 47(4), 385-392. DOI: 10.5658/WOOD.2019.47.4.385
- Zhao, P., Dou, G., and Chen, G. S. (2014). "Wood species identification using improved active shape model," *Optik* 125(18), 5212-5217. DOI: 10.1016/j.ijleo.2014.06.047

Article submitted: May 17, 2021; Peer review completed: August 14, 2021; Revised version received: October 8, 2021; Accepted: December 17, 2021; Published: January 5, 2022.

DOI: 10.15376/biores.17.1.1187-1204

APPENDIX

Table S1. Latin Names and Densities of Species

| | Latin Name | Mean of Density | Standard Deviation |
|----|--|-----------------|--------------------|
| 1 | <i>Pterocarpus macrocarpus</i> | 1.165 | 0.039 |
| 2 | <i>Pterocarpus pedatus</i> | 1.103 | 0.043 |
| 3 | <i>Pterocarpus erinaceus</i> | 0.929 | 0.020 |
| 4 | <i>Dalbergia latifolia</i> | 0.920 | 0.030 |
| 5 | <i>Dalbergia frutescens</i> var. <i>tomentosa</i> | 1.303 | 0.054 |
| 6 | <i>Pterocarpus indicus</i> | 0.448 | 0.050 |
| 7 | <i>Dalbergia melanoxyton</i> | 1.212 | 0.047 |
| 8 | <i>Dalbergia cochinchinensis</i> | 1.207 | 0.028 |
| 9 | <i>Dalbergia bariensis</i> | 1.109 | 0.036 |
| 10 | <i>Dalbergia oliveri</i> | 1.029 | 0.017 |
| 11 | <i>Dalbergia retusa</i> | 1.112 | 0.026 |
| 12 | <i>Millettia stuhlmannii</i> | 0.704 | 0.026 |
| 13 | <i>Dalbergia louvelii</i> | 0.891 | 0.045 |
| 14 | <i>Dalbergia cultrata</i> | 0.982 | 0.028 |
| 15 | <i>Baphia nitida</i> | 1.285 | 0.043 |
| 16 | <i>Swartzia madagascariensis</i> | 1.083 | 0.028 |
| 17 | <i>Pterocarpus tinctorius</i> | 0.993 | 0.028 |
| 18 | <i>Myroxylon balsamum</i> | 0.940 | 0.040 |
| 19 | <i>Pterocarpus soyauxii</i> | 0.730 | 0.020 |
| 20 | <i>Dipteryx</i> sp. | 0.987 | 0.024 |
| 21 | <i>Vatairea</i> sp. | 0.867 | 0.038 |
| 22 | <i>Pericopsis elata</i> | 0.660 | 0.018 |
| 23 | <i>Pterocarpus angolensis</i> | 0.595 | 0.010 |
| 24 | <i>Platymiscium</i> sp. | 1.062 | 0.035 |
| 25 | <i>Andira</i> sp. | 0.766 | 0.025 |
| 26 | <i>Diplotropis</i> sp. | 0.814 | 0.033 |
| 27 | <i>Machaerium</i> sp. | 1.036 | 0.037 |
| 28 | <i>Swartzia leiocalycina</i> | 1.268 | 0.042 |
| 29 | <i>Baphia kirkii</i> | 1.104 | 0.030 |
| 30 | <i>Dalbergia cearensis</i> | 0.764 | 0.041 |
| 31 | <i>Dalbergia tucurensis</i> | 0.706 | 0.037 |
| 32 | <i>Cylicodiscus gabunensis</i> | 0.838 | 0.043 |
| 33 | <i>Marmaroxylon racemosum</i> | 0.934 | 0.048 |
| 34 | <i>Xylia</i> sp. | 0.989 | 0.052 |
| 35 | <i>Samanea saman</i> | 0.650 | 0.038 |
| 36 | <i>Anadenanthera macrocarpa</i> | 0.964 | 0.036 |

| | | | |
|----|-----------------------------------|-------|-------|
| 37 | <i>Acacia sp.</i> | 1.035 | 0.032 |
| 38 | <i>Pinus sp.</i> | 0.478 | 0.045 |
| 39 | <i>Pinus sylvestris</i> | 0.532 | 0.030 |
| 40 | <i>Pinus sp.</i> | 0.654 | 0.024 |
| 41 | <i>Pseudotsuga sp.</i> | 0.452 | 0.033 |
| 42 | <i>Tsuga sp.</i> | 0.386 | 0.037 |
| 43 | <i>Pinus radiata</i> | 0.427 | 0.034 |
| 44 | <i>Cassia siamea</i> | 1.041 | 0.038 |
| 45 | <i>Colophospermum mopane</i> | 1.298 | 0.047 |
| 46 | <i>Guibourtia tessmannii</i> | 0.805 | 0.022 |
| 47 | <i>Microberlinia sp.</i> | 0.909 | 0.032 |
| 48 | <i>Paraberlinia bifoliolata</i> | 0.676 | 0.040 |
| 49 | <i>Intsia sp.</i> | 0.902 | 0.032 |
| 50 | <i>Peltogyne sp.</i> | 1.168 | 0.044 |
| 51 | <i>Caesalpinia paraguariensis</i> | 1.108 | 0.010 |
| 52 | <i>Erythrophleum fordii</i> | 0.989 | 0.037 |
| 53 | <i>Daniellia sp.</i> | 0.525 | 0.025 |
| 54 | <i>Guibourtia conjuata</i> | 1.084 | 0.042 |
| 55 | <i>Berlinia sp.</i> | 0.673 | 0.032 |
| 56 | <i>Koompassia sp.</i> | 0.623 | 0.040 |
| 57 | <i>Sindora sp.</i> | 0.623 | 0.046 |
| 58 | <i>Dicorynia sp.</i> | 0.721 | 0.025 |
| 59 | <i>Martiodendron sp.</i> | 0.881 | 0.028 |
| 60 | <i>Vouacapoua americana</i> | 0.942 | 0.025 |
| 61 | <i>Hymenaea sp.</i> | 0.795 | 0.037 |
| 62 | <i>Azelia sp.</i> | 0.889 | 0.033 |
| 63 | <i>Guibourtia coleosperma</i> | 0.962 | 0.023 |
| 64 | <i>Erythrophleum sp.</i> | 0.736 | 0.012 |
| 65 | <i>Cynometra sp.</i> | 0.957 | 0.020 |